Contents of this file

Additional Supporting Information (Files uploaded separately)

Introduction

The supporting information for this manuscript includes one supplementary text section, five supporting figures (referenced in the main manuscript) and three supporting tables. Data types and processing are as indicated in the main manuscript text.

Section S1

Informal discussions with a colleague had raised the possibility that freeze drying sediments caused the breakage of foraminifera tests due to the intensity of the vacuum and the very cold temperatures employed. To test this hypothesis, we undertook an experiment to specifically evaluate whether the percent coarse fraction (%CF) was influenced by the sediment drying method employed. We dried aliquots of six samples overnight using both a conventional oven at 45°C and a freeze drier at -50°C. The data from that experiment are shown in Figure S1. The average difference between the two drying methods, over six different depth intervals (n=12), was ~0.66% and there are no statistically significant offsets between the two methods (p-value >0.05). We interpret these data as indicating no significant differences between the two methods and all other samples referenced in the manuscript were freeze dried and then sieved to determine %CF.
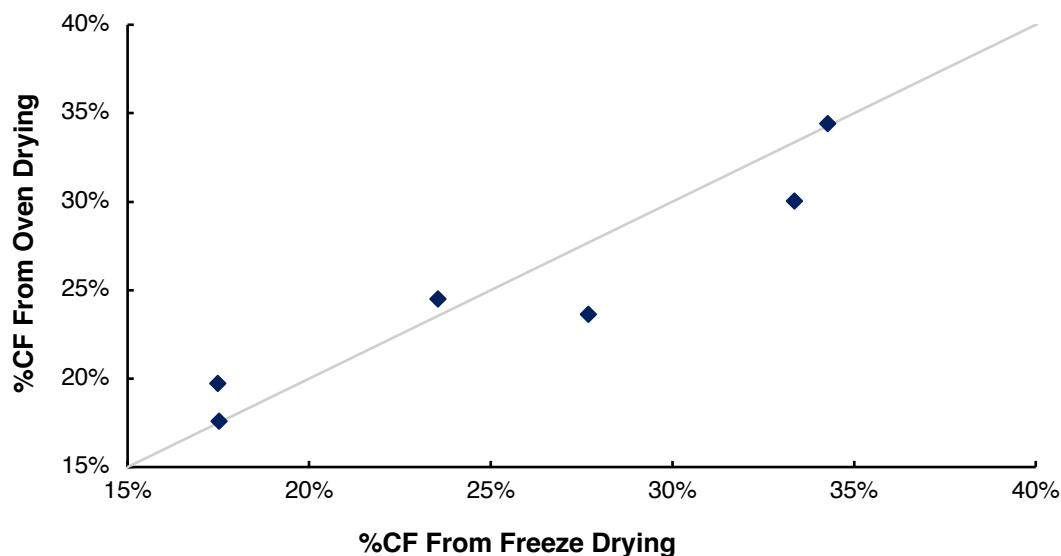
Figure S1. Data from the experiment to test two different methods of sample drying. Blue diamonds indicate the %CF derived from paired samples that were freeze dried and oven dried. The solid grey line indicates the 1:1 line. The Pearson Correlation is 0.94 and the p-value for the one-tailed t-test is 0.26.
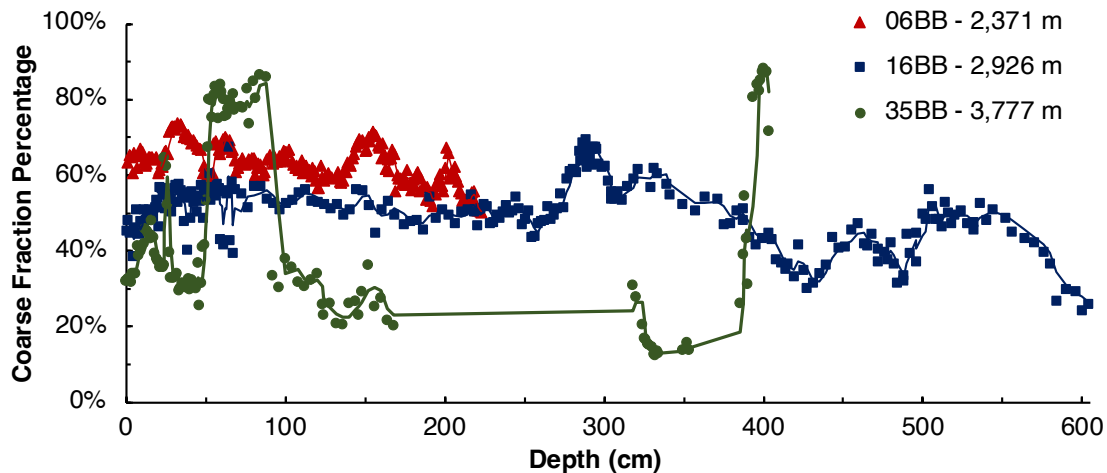

Figure S2. Coarse fraction percentage data from the three cores that are the focus of this study 06BB (red triangles), 16BB (blue squares), and 35BB (green circles). Lines represent a three point moving average for each dataset.
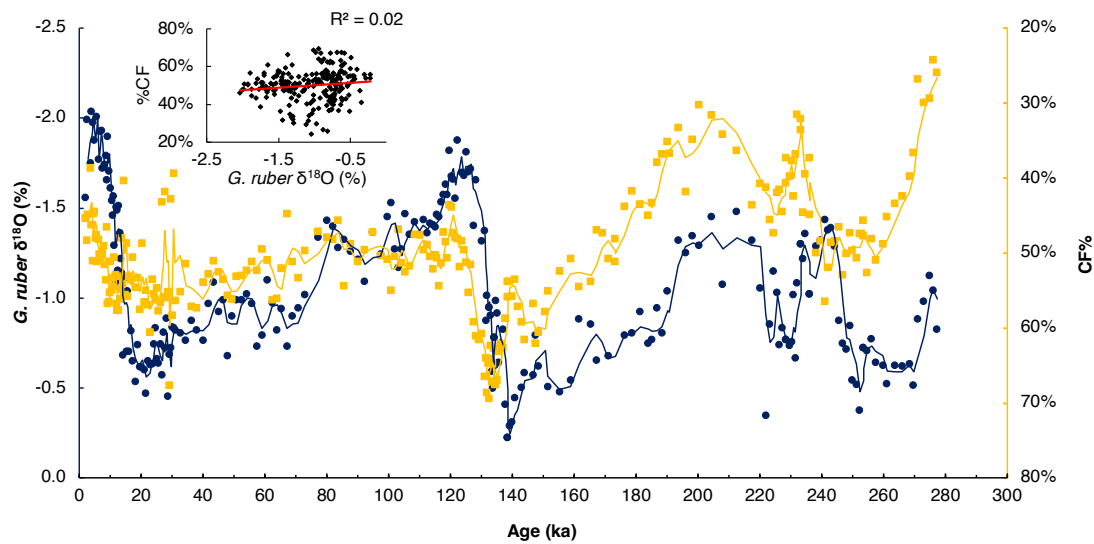
Figure S3. Coarse fraction percentage (gold squares) and *G. ruber* oxygen isotope data (navy circles) from core 16BB. Note the inverted axis for coarse fraction percentage. Inset shows the linear regression of the two datasets with an r^2 of 0.02.

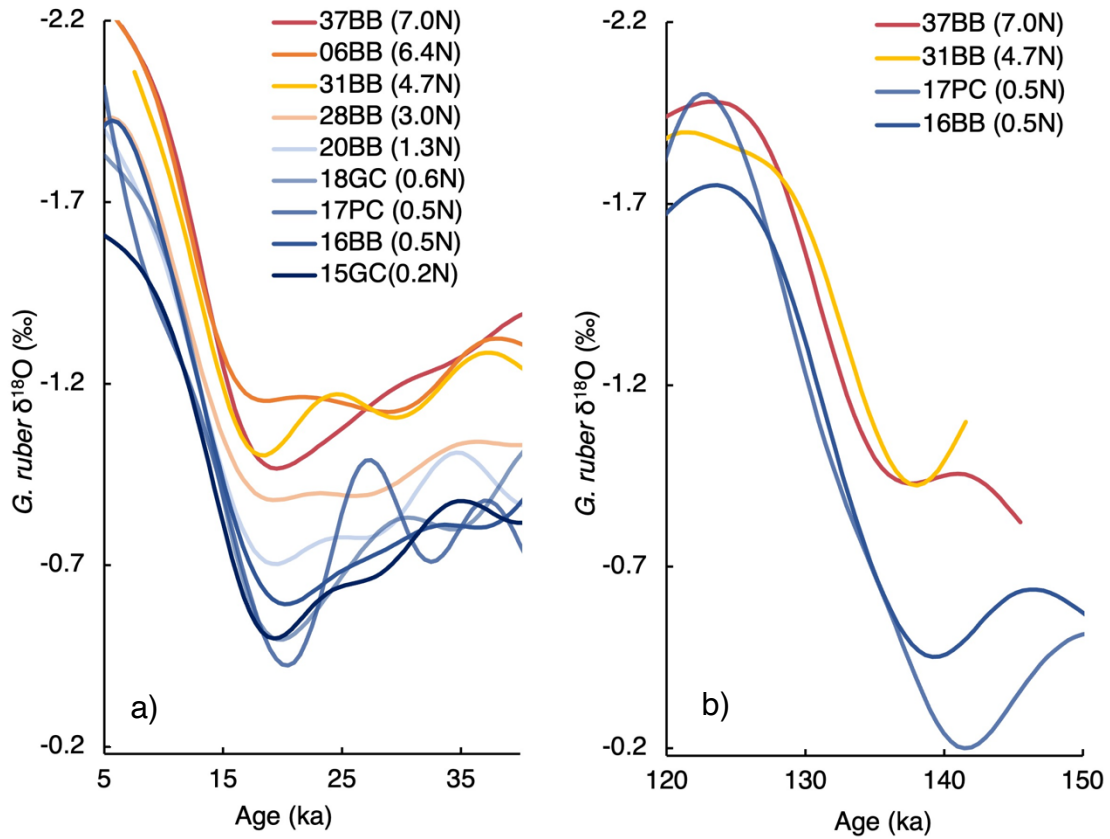**Figure S4. ML1208 Planktonic Oxygen Isotope Gradients.** Bandpass filtered records of *G. ruber* δ^{18}O from ML1208 cores as in main text Fig. 6 with a focus on a) the LGM to Holocene (last deglaciation) and b) MIS6-5 (penultimate deglaciation). Note that the y-axes of the two panels are the same for comparison.
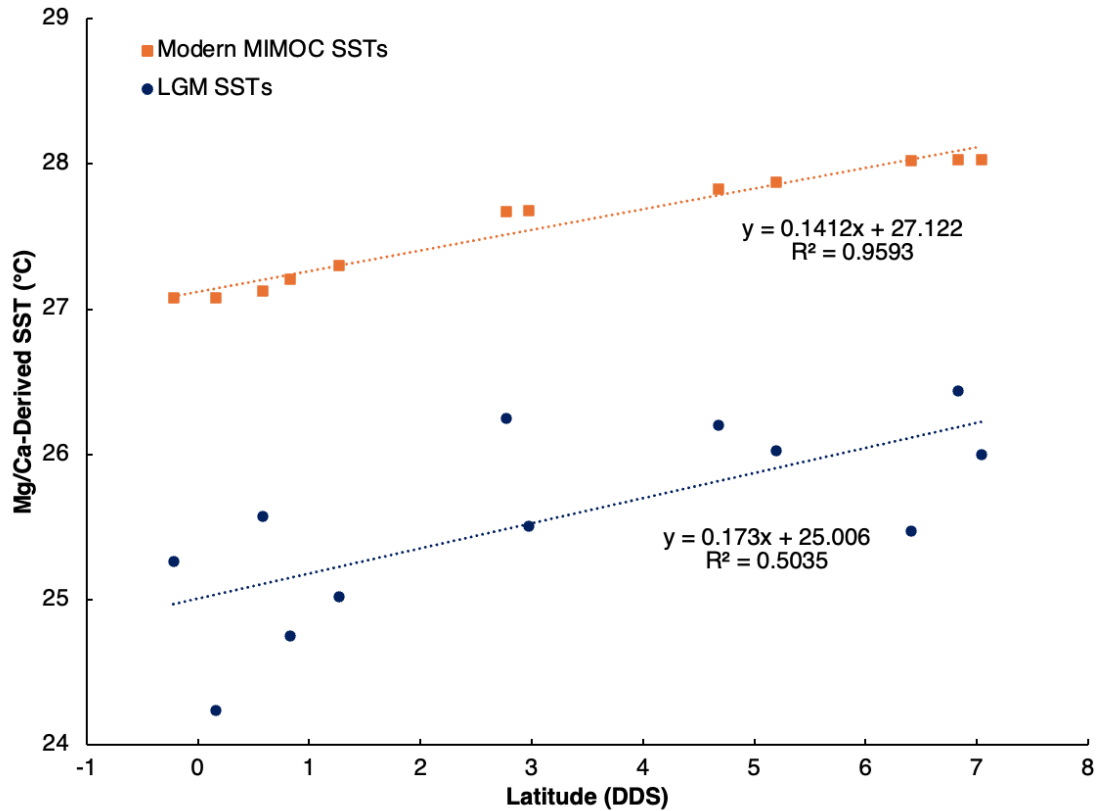
Figure S5. Sea Surface Temperature (SST) data derived from Mg/Ca from Monteagudo et al., 2021. The lines of best fit and Pearson Correlation Coefficients for the modern SSTs (orange squares) and LGM SSTs (navy circles) are as illustrated on the figure. Both datasets have statistically significant slopes, however the slopes are not statistically distinguishable at the p=0.05 level. These lines of best fit differ from those originally published by Monteagudo et al. who used two different line segments (break at 2°N) to describe the LGM data.

--

(Table S1 uploaded separately)

Table S1. All published radiocarbon dates from the Line Islands cores. Data have been recalibrated using the parameters indicated in the text.

Core	Latitude (DDS)	Longitude (DDS)	Water Depth (m)	Holocene SR	Holocene SR 1σ	LGM SR	LGM SR 1σ	MIS5 SR	MIS5 SR 1σ	MIS6 SR	MIS6 SR 1σ	MIS7 SR	MIS7 SR 1σ	MIS8 SR	MIS8 SR 1σ	MIS9 SR	MIS9 SR 1σ
'37BB'	7.04	-161.63	2798	2.41	0.34	1.08	0.14	0.78	0.10	2.12	0.12						
'06BB'	6.41	-161.01	2371	3.03	1.05	2.65	0.09										
'31BB'	4.68	-160.05	2857	4.71	0.70	2.21	0.08	2.74	0.04	7.29	0.16						
'28BB'	2.97	-159.20	3153	3.60	0.07	2.72	0.15										
'20BB'	1.27	-157.26	2850	2.71	0.14	3.29	0.07										
'18GC'	0.59	-156.66	3362	4.37	0.12	4.13	0.07										
'16BB'	0.48	-156.45	2926	2.87	0.06	1.50	0.10	2.89	0.04	3.07	0.10	1.68	0.07	2.88	0.09		
'17PC'	0.48	-156.45	2926	5.10	0.41	2.45	0.06	1.99	0.08	2.58	1.12	1.79	0.15	2.81	0.50	1.70	0.06
'15GC'	0.16	-156.12	3597	2.96	0.38	3.72	0.07										

Table S2. Average sedimentation rates (SR) and 1σ uncertainties in units of cm/ka calculated over selected time slices for ML1208 cores. Holocene (2-8 ka) and LGM (18-24 ka) time slices, with values and additional time slice data for MIS5 (120-126 ka), MIS 6 (138-144 ka), MIS 7 (236-242 ka), MIS 8 (248-254 ka) and MIS 9 (326 –332 ka).

Core	Latitude (DDS)	Longitude (DDS)	Water Depth (m)	Holocene δ^{18}O (‰)	LGM δ^{18}O (‰)	LGM-Holocene δ^{18}O (‰)	MIS5 δ^{18}O (‰)	MIS6 δ^{18}O (‰)	MIS6-5 δ^{18}O (‰)	MIS7 δ^{18}O (‰)	MIS8 δ^{18}O (‰)	MIS8-7 δ^{18}O (‰)	MIS9 δ^{18}O (‰)
'37BB'	7.04	-161.63	2798	-2.19	-0.97	1.22	-1.97	-0.88	1.09				
'06BB'	6.41	-161.01	2371	-2.24	-0.86	1.38							
'31BB'	4.68	-160.05	2857	-2.06	-0.96	1.10	-2.15	-0.71	1.44				
'28BB'	2.97	-159.20	3153	-1.94	-0.81	1.13							
'20BB'	1.27	-157.26	2850	-1.99	-0.62	1.37							
'18GC'	0.59	-156.66	3362	-1.90	-0.38	1.52							
'16BB'	0.48	-156.45	2926	-2.06	-0.47	1.59	-1.88	-0.23	1.65	-1.44	-0.38	1.06	
'17PC'	0.48	-156.45	2926	-2.02	-0.41	1.62	-2.13	-0.02	2.12	-1.57	-0.15	1.42	-1.67
'15GC'	0.16	-156.12	3597	-1.64	-0.38	1.26							

Table S3. *G. ruber* δ^{18}O (‰) minima (interglacial) and maxima (glacial) values computed over selected time slices for ML1208 cores. Time slices as described in manuscript and Table S2 above.